# Carbon ion dosimetry on a fluorescent nuclear track detector using widefield microscopy

*Dietrich W.M. Walsh[1], Hans Liew[1], Julian Schlegel[1], Andrea Mairani [2-5], Amir Abdollahi [2-5], Martin Niklas[1],*

1 *Clinical Cooperation Unit Translational Radiation Oncology, National Center for Tumor Diseases (NCT), Heidelberg University Hospital (UKHD) and German Cancer Research Center (DKFZ), Heidelberg, Germany*

2 *Division of Molecular and Translational Radiation Oncology, Department of Radiation Oncology, MFHD and UKHD, Heidelberg Ion-Beam Therapy Center (HIT), Heidelberg, Germany*

3 *German Cancer Consortium (DKTK) Core-Center Heidelberg, DKFZ, Heidelberg, Germany*

4 *Heidelberg Institute of Radiation Oncology (HIRO), National Center for Radiation Oncology (NCRO), Heidelberg University and DKFZ, Heidelberg, Germany*

5 *Heidelberg Ion-Beam Therapy Center (HIT), Heidelberg, Germany.*

**Abstract**

Fluorescent nuclear track detectors (FNTD) are solid-state dosimeters used in a wide range of dosimetric and biomedical applications in research worldwide. FNTD's are a core but currently underutilized dosimetry tool in the field of radiation biology which are inherently capable of visualizing the tracks of ions used in hadron therapy. The ions that traverse the FNTD deposit their energy according to their linear energy transfer (LET) and transform colour centres to form trackspots around their trajectory. These trackspots are the fingerprints of the ions which have fluorescent properties (620 nm peak excitation and 750 nm emission). These properties enable an analysis of the trackspots in the FNTD using fluorescence microscopy enables a well-defined dosimetric readout with a spatial component indicating the trajectory of individual ions. The current method used to analyse the FNTDs is laser scanning confocal microscopy (LSM). This imaging technique enables a precise localization and imaging of track spots in x, y and z however due to the scanning of a single laser spot across the sample requires a lot of time for large samples. This body of work conclusively shows for the first time that the readout of the trackspots present after irradiation (0.5 Gy carbon ions) in the FNTD can be captured with a widefield microscope (WF). This method was developed to optimize the readout of the *Cell-FIT-HD* biomedical sensor based on a Landauer $Al_2O_3$:C,Mg FNTD which is used for biological single cell dosimetry and tracking using widefield microscopy. The cells to be analysed are seeded onto an FNTD and irradiated with carbon ions, then the FNTD and the cells can be imaged using an LSM and the WF microscope respectively. The capture of the two separate readouts, cells and tracks, on two separate microscopes is not only time intensive but also introduces a spatial error between tracks and cells which needs to be corrected. The work in this paper now enables the use of a single widefield microscope to image the cells growing on the FNTD and the tracks in the FNTD. In comparison to the current LSM system the WF readout of the FNTD is a factor ~10 faster, for an area 2.97 times the size making the method nearly a factor 19 faster in track acquisition. This WF setup will replace LSM in the *Cell-FIT-HD* for FNTD track readout, which will enable a higher throughput of samples as well as a reduced error in the correlation between tracks and cells and enable a high throughput readout of *Cell-FIT-HD.*

## Introduction

Fluorescent nuclear track detectors (FNTD) are widely used in radiation dosimetry and radiation biology applications to detect and quantify the energy and trajectory of particles from neutrons to heavy ions [1]. Their usage spectrum spans from quality control of microbeams [2] to neutron dosimetry [3]. One of the most promising current applications in research however is the use of FNTDs for heavy ion beam therapy research. The widespread use of radiation as a therapeutic modality in oncology and the increasing number of hadron therapy centers opening worldwide [4] has lead to the increased interest in the fundamental response of cells to ion irradiation. In the field of fundamental radiation research FNTDs are becoming a truly valuable tool [1]. One such implementation for biomedical radiation research is the **Cell F**luorescent **I**on **T**rack **H**ybrid **D**etector (*Cell-FIT-HD*) biomedical sensor used for in situ biodosimetric detection of single ion traversals in cells irradiated with heavy ions (Fig.1) [5]. The biomedical sensor is based on a Landauer $Al_2O_3$:C,Mg FNTD [6, 7]. Cells are grown on the FNTD and irradiated with ions and their response is then analysed. The ions traversing the cells and the FNTD induce transformation of colour centres visible as track spots along the particles track. These trackspots can be used to reconstruct the particles trajectories through the FNTD and cell layer in order to perform single cell bio dosimetry down to the subcellular level [8, 9]. Cells expressing genetically encoded DNA damage markers such as 53BP1 growing on an FNTD can then be imaged after irradiation to asses the relation of ion hits to DNA foci [10, 11]. Furthermore live cell imaging approaches after ionizing radiation can be used to determine the individual cell fate [12].

The current standard for the dosimetric readout method for the Landauer $Al_2O_3$:C,Mg FNTD is confocal laser scanning microscopy (CLSM) [9, 13]. LSM enables precise scanning and detection of fluorescence signal in well-defined optical z-sections. Scanning a high intensity laser over a sample and rejecting out of plane light by an adjustable pinhole before detection by a fast avalanche photodiode is ideal for acquiring signal from the weakly fluorescent tracks in the FNTD. It is however a slow process which limits the size of the field and the resolution to be captured. Due to the high laser intensity and the time required to image a field at a high resolution the LSM is less suitable for experiments where live cells are imaged on the FNTD for days as the cells are more likely to suffer from phototoxic damage. In contrast, the ideal imaging setup for live cell imaging of cells growing on the FNTD is a widefield microscope (WF) combined with a high sensitivity sCMOS camera as this enables a larger number of frames to be acquired over time and using a tunable LED excitation and a live cell incubation chamber can insure minimal phototoxicity and cellular viability. The current readout process of *Cell-FIT-HD* for example uses two microscopes to perform in situ bio dosimetry, the imaging routine used to detect the ionizations in an irradiated FNTD makes use of a Zeiss LSM710 confocal microscope [14-16]. The second microscope used to image the cells growing on the FNTD was

an Olympus IX83 widefield microscope with LED illumination and live cell incubation chamber is used to ensure the cells are growing at a constant 37°C and 5% CO2.
The experimental procedure of *Cell-FIT-HD* requires cells to be plated on an FNTD which is irradiated at the Heidelberg Ionenstrahl Therapiezentrum (HIT), then within 5-10 minutes, transferred to the widefield microscope where an initial image for cell position and ion traversal cross-referencing is captured. Then the cells are observed for up to 4 days using a variety of imaging methods to analyse the individual cells response to heavy ion irradiation [12]. After the live cell imaging the FNTD is transferred to the LSM where the fluorescent colour centres caused by the traversing ions can be detected. The FNTD images are then retrospectively registered with the initial images taken after irradiation to cross reference the hits to the location of the cells [16].
The readout of the ionization tracks in the FNTD by LSM is currently performed after imaging of the cells growing on the FNTD has been completed. The imaging of the sample on two microscopes adds spatial uncertainty, on the scale of 1 µm which is rectified by a subsequent image registration of the field of view (FOV) from widefield to confocal [16]. However, the registration of the images between the two microscopes introduces an uncertainty to the ion traversals relative to the cells [16]. The readout of one FNTD FOV stack of 20 images (193x193um, 1024x1024px 8-bit image, 40X objective) via LSM takes ~11 minutes using a Zeiss CLSM710. In order to simplify and greatly accelerate the image acquisition and reduce the sources of error the main aim of this work was to use a single widefield microscope to enable the imaging of both the cells on the FNTD and the tracks in the FNTD. To ensure the FNTD readout on the widefield microscope yielded the expected number of ion traversals the data was compared to monte carlo (FLUKA) simulations of the irradiation performed at HIT.

## Methods

### Irradiation of the FNTD

The FNTDs analysed in this paper were irradiated at Heidelberg Ionenstrahl Therapiezentrum (HIT) with 0.5 Gy carbon ions at 3.5cm depth in a 3-4cm spread out bragg peak (SOBP). Irradiation setup was similar to the setup used in [15]. The irradiated FNTD was the physical compartment of the biomedical sensor Cell-Fit-HD$^{4D}$ introduced in [12]: Briefly, the bottom of a conventional 6 well glass bottom dish (MatTek) was replaced by a disk-shaped FNTD (diameter: 19 mm, thickness: 100µm, Fig.1). The resulting irradiated FNTDs were then stored in the dark until further analysis. The dose uncertainty is taken as 5% for a field of 1x1cm, therefore 0.5 Gy +-0.025 Gy.

### Microscopy and image analysis

The FNTD readout was performed on an Olympus IX83 widefield microscope. The Olympus IX83 was equipped with a Hamamatsu Orca flash 4.0 v2 sCMOS detector (Peak Quantum efficiency 82% at 650nm) and a lumencore SpectraX LED illumination system. The sample was excited with a 640/30nm LED at 100% LED intensity (231 mW) using a Plan-Apochromat 40x/1.4 Oil DIC M27 objective. The exposure time was set to 5 seconds and binning 1 x 1, the resolution of the detector was 2048x2048 with an image field of view of 333 x 333 µm. The emission filter was a chroma “lumencore X” multi-emission filter with an emission filter for the range of interest (670-760nm). The images acquired were 16bit. Before imaging a flat field correction was performed using a Chroma slide and the Olympus CellSens Software (version 1.15) to ensure flat images.
The IX83 was used to image a 0.5 Gy carbon ion irradiated FNTD. The resulting WF images were analysed using the FNTD analysis software developed and implemented in ImageJ [13, 17]. To ensure that no bias or artifacts were introduced into the analysis, the raw data was

used. No background correction or signal filtering was performed except for a simple intensity thresholding (MOSAIC Feature point detection parameter: Threshold 0.1-0.17) for the individual track spots in the FNTD imageJ macro. The result of which is a dramatic reduction in non-primary ion track detection. The resulting track spots were reconstructed over the z-axis by the software and exported to csv. Histogram Plots of the mean track intensity (entry "mean.int") of valid tracks were plotted in using the software Rstudio [18]. These plots formed the basis of the particle distribution analysis.

**Calculation of Trajectory LET**

The $LET$ of the individual trajectories were determined based on the measured fluorescence intensity of the trajectories, $I$, using the following Equation.

*Eq.1:*

$$LET = 10^{\frac{I}{a}} - b,$$

Where $a$ and $b$ are free parameters [9]. In this work, $a$ and $b$ were optimized manually with the objective to achieve maximum overlap of the measured intensity and simulated LET spectrum (Fig. 4B).

**Monte Carlo simulation (FLUKA)**

Monte Carlo simulation for the Carbon ion irradiation performed at HIT was simulated for a SOBP at 3.5cm depth and a field of about 13 cm x 9 cm. The FLUKA Monte Carlo version fluka.2011.2x.8 has been used. In terms of settings, the default ones employed for hadron therapy application has been used as described in [15, 19]. A detailed geometry of the HIT beam-line was implemented. In order to get enough statistics, about 1% of the planned particle fluence has been simulated, i.e. 7.69380e+06. In order to access the information (charge, mass, energy per nucleon and LET ) of the particles crossing the detector, we have implemented an event-by-event read-out of MC simulations allowing us to use the same reconstruction constraints in both the simulation and in the experimental data. The monte carlo simulation of the particle irradiation performed in FLUKA yielded a total particle fluence of 1.54e+07 for 1 Gy. The fluence consisted of carbon, beryllium, boron, helium and proton counts. For LET calculations in water, for each particle traversal (Z,A) at a certain energy per nucleon, the corresponding LET value is sampled on-line using FLUKA internal routine.

(from andrea)

**Results**

FNTDs Irradiated with 0.5 Gy carbon ions (SOBP width 3-4cm) were imaged using the WF microscope and the data analysed to determine the track spots of the primary particles (carbon ions) using the FNTD analysis package [13]. The first image stacks captured with widefield showed that it was possible to detect and reconstruct ion tracks using the widefield system (Fig.2). Ionization tracks created by the carbon and secondary ions (Be, B, He, P) in the irradiation field in the FNTD were visualized with the widefield system. When compared to FLUKA simulations it was clear that neither the LSM or the WF were capable of imaging all of the secondary particle species which were expected to be seen based on the monte carlo simulation. As the dose deposited in the cells by the primary carbon ions accounts for 93.4% of the total dose it was therefore decided to focus on the detection of the carbon ions as these cause for the majority of the dose and can all be detected unlike the secondaries. MC simulated carbon ion fluence for the 0.5 Gy irradiation plan was calculated to be 4.165e+06 $cm^{-2}$, in comparison the measured fluence in the FNTD as

measured by WF was 4.452e+06 $cm^{-2}$ (mean of three 333x333 µm FOV images measured) there is therefore still an overestimation off around 10%.
The WF datasets were qualitatively comparable to the images produced by the LSM in relation to their signal distribution and track spots (Fig.2B). The exposure time on the sCMOS (widefield) was increased to 5 seconds to ensure the largest possible dynamic range of the detector could be used while reducing acquisition time. The use of a high quantum efficiency and low dark current sCMOS detector (Hamamatsu Orca Flash v2) on the widefield microscope enabled the more rapid acquisition of the z-stack (21 slices) than possible on the confocal for a larger field of view (FOV). The difference in acquisition time was nearly a factor 10 faster (1 minute 45 seconds) for a 333 x 333 µm field at 2048 x 2048 pixels, acquired with WF, when compared to a 193 x 193 µm field with 1024 x 1024 pixel confocal field (11 minutes). The area acquired by WF is therefore 2.97 time larger than that of LSM. Therefore the acquisition of the tracks in the wafer can be acquired up to ~19x faster using WF.
A significant difference in the analysis step is the background correction. The images taken on the WF microscope can be analysed by the FNTD macro in their raw unaltered state with no background correction or signal modification and yield excellent results, for primary particles. The reconstruction of the ion tracks using the ImageJ package shows that the quality of the WF images were ideally suited for an analysis of the particle tracks without applying any image filtering or background correction to the raw data. The data were merely thresholded during track analysis to minimize the detection of secondary particles (proton, helium, boron and beryllium). The threshold used was integrated in the FNTD package, the three chosen threshold values were plotted in R (Fig.3). A value of 0.17 (MOSAIC Feature point detection parameter: Threshold) was determined to fulfill the criteria well.
To verify the Linear Energy Transfer (LET) distribution of the primary carbon ions in the FNTD the images of the 0.5 Gy carbon ion irradiated FNTD were compared to the results from FLUKA simulation data for the same irradiation. To compare the two distributions the raw FNTD track data were analysed and the threshold was set (MOSAIC threshold value 0.17) to exclude the majority of secondary ions without changing the distribution of primary ions. The FLUKA simulation data for primary carbon ions was calculated for 1 $cm^2$, this was first normalized to the area microscope FOV (333x333) then using Eq.1 the LET of the individual trajectories was calculated and (measured track intensity vs FLUKA) were fitted in matlab (Fig.4B). The resulting graph shows a high degree of overlap of the two curves and a calculated dose of 0.52 Gy (carbon ions) from the measured track spots. The applied physical dose for the FNTD in question was 0.5 Gy (SOBP, all particles) with a dose uncertainty of 5%. The dose contributed by carbon ions alone was calculated to be 0.467 Gy (from FLUKA, carbon ions contribute 93.4 % of the dose) The detection mismatch between the planned physical dose of carbon ions (FLUKA) and the detected carbon ion dose (FNTD) for one analyzed field (333x333 µm) is therefore 8.9 % for the settings chosen.
In addition to the fast readout time and the excellent signal which can be acquired from the Irradiated FNTDs using WF imaging an additional interesting background signal was detected. When the exposure time was set to 10 seconds (maximum setting for the sCMOS) a unique signal appeared in all slices of the 21 z-stack layers. Fig.6 depicts the background signal found in the FNTD which may, due to the sheer number of snake like tracks be secondary electrons which transform colour centres within the FNTD. This layer is visibly above background and shows a distinct short snake-like pattern throughout the FNTD. These tracks covered the whole irradiated area of the FNTD and were a strong first indication that the FNTD is inherently capable of detecting secondary electrons. The detection and analysis of these signals was however not further followed in this work.

**Discussion and Conclusion**

Confocal microscopy is currently the standard method for FNTD track readout. The ability to detect light from highly defined z-planes along with the excellent signal to noise ratio situated confocal microscopy as an ideal tool for FNTD readout. However, when using the FNTD as the physical compartment in the biosensor *Cell-FIT-HD* to monitor cells for days after irradiation using WF live cell imaging the confocal system adds additional time constraints and more sources of error to the readout process, thus limiting the ability of *Cell-FIT-HD* to be a high throughput system when working with cells. The main downside of the current readout system is that two microscopes are required, one for live cell imaging, the second for the FNTD readout and therefore the FNTD needs to be transferred to a new microscope after biological imaging for colour center imaging. The registration of track images and cell images captured on the two separate systems introduces a spatial error with regard to the ion track to cell reconstruction. As the images are captured separately on two different occasions and on two different microscopes the field reconstruction is time consuming and involves manually identifying microscopy fields by the inherent colour centre defects in the FNTD [16]. The increased time and effort required to gain an increase in z-axis resolution during FNTD readout along with the fact that the use of two microscopes introduces errors in relation to the captured FOV and the required imaging time strongly diminishes the use of the confocal system[16]. The WF readout however does require longer exposure times for each field of up to 5s. In addition it requires a well calibrated and flatfield corrected image to work well in addition to a sensitive modern sCMOS sensor.

In this paper it has been shown for the first time that by using a widefield microscope with a high quantum efficiency sCMOS sensor and a defined excitation LED system both the FNTD colour centres (tracks) and the cells can be imaged by a single system. The WF Images gained from the FNTD are very similar or in some cases even better than those gained from the confocal system and can be acquired a factor 20 faster. The larger sensor also enables a larger FOV which is 2.97x larger compared to the LSM images, when taken into account the WF method is therefore ~19x faster than LSM. The WF readout setup does not introduce any further spatial errors as the sample stays in the same microscope and is therefore only limited by the precision of the stage. The resulting WF images from the sCMOS detector have a very similar signal quality with far less optimization steps required (scan frequency, dwell time, pinhole settings) which enables a faster and more reproducible readout. The WF readout method is not meant to replace the LSM readout as it has a reduced z-resolution and cannot reach the same signal to noise ratio as is possible with an in-depth LSM readout. This would be required for more dosimetrically demanding tasks such as neutron dosimetry. However its major advantage is the simple setup with comparatively few settings needed to be optimized and the dramatic decrease in time required to capture the stacks required for ion track analysis.

When comparing the expected number of primary carbon ions and their LET simulated by FLUKA (for a 333x333um area) with the detected number of particles and their energy distribution the results indicate a calculated dose difference of 8.9% between FLUKA and FNTD output for a single field. One of the possible sources for the dose mismatch could be the thresholding and image analysis methods used during the image analysis. Background correction (as used for LSM images) and image correction methods currently used in the FNTD package for LSM and WF may lead to a less accurate detection of primary particles. It is currently not possible to remove all secondary tracks while preserving all primary tracks which leads to an altered number of tracks and ions detected which in turn will lead to a

change in dose. In addition to the reduced spatial error and decreased acquisition time when using WF there is evidence that it is now possible to detect a secondary background signal using the WF system (Fig.6), however the source of these signals still needs to be verified and quantified before it can be uniquely identified as being from any one source.
In this body of work the choice was made not to compare LSM and WF in a quantitative manner. The method for LSM analysis which is in use requires varying levels of image correction and filtering, unlike the WF imaging method where the raw flat-fielded images are used. This would require an image by image subjective thresholding and optimization procedure of the LSM datasets. As the data being compared would therefore not be similar and the raw LSM data are currently not suited for analysis, we decided such a comparison would reduce the scientific accuracy of the work. It is therefore important to note that this paper does not look to replace LSM imaging as a method for FNTD analysis but to introduce a further option for experiments where other factors, such as time, limit the microscopic analysis.
In conclusion, it has been shown that it is now possible to image ion tracks in an FNTD using a WF microscope. The method will enable the use of a single widefield microscope to analyse both cells growing on, and the tracks induced by primary ions in an irradiated FNTD (in the *Cell-FIT-HD* biosensor). The images from the widefield are ideally suited for primary ion track reconstruction while requiring up to a factor ~19 less time to acquire. The new process simplifies image reconstruction and will enable the future analysis of cells and FNTD on a single widefield microscope. The significant time saving and reduction in spatial error will enable a higher throughput of cells and the analysis of more ionization tracks and cells, which will enable an even more robust statistical analysis in the future when using the *Cell-FIT-HD* biosensor for radiobiological experiments.

**Figure Legends**

Figure 1.
A simplified overview of the biomedical sensor *Cell-FIT-HD*. Upper image is a modified 6 well plate with 19mm diameter FNTDs (FNTD in shape of a wafer 100µm thickness) inserted (*) used for growth of cells during live cell imaging. The three diagrams in the centre and the two corresponding micrographs depict the process of irradiation (Left), live cell imaging of cells (Centre) and trackspot imaging (including image registration, Right). Overview of workflow of *Cell-FIT-HD* was adapted from Manuscript bioarchive, representations of FNTD adapted from [12]. Scale bars represent 10 µm.

Figure 2.
Overview of the image stacks captured using the LSM and widefield microscopes of the same 0.5Gy Carbon ion irradiated FNTD. (A) Direct qualitative comparison of image stacks taken with confocal and widefield microscopes, two stacks with 21 slices were captured, the details are listed below each image. (B) A representative image captured with LSM and WF using 40X objectives (upper). The 3D signal peaks are taken from the marker areas and show very similar morphology (lower). The CLSM image is 8 bit and the WF image is 16 bit.The scale bars represent 5 and 10 µm respectively in A and B

Figure 3.

Histograms of four different threshold values used for Carbon ion track reconstruction threshold testing. The four graphs show the distribution of track intensity and frequency for varying threshold values (0.11-0.17, FNTD analysis software). When analyzing the tracks in the FNTD with the FNTD package in imageJ a MOSAIC threshold value must be set, to ensure the least amount of secondary particles are included in the analysis. To define an ideal threshold, different thresholds were tested and the resulting track spot histograms plotted in Rstudio. The graphs show that with increasing threshold value the secondary peak, left in all graphs, shrinks as the value is increased while the primary peak , right, stays unchanged. The value of 0.17 was chosen for further Primary particle analysis.

Figure 4.

Figures show the Monte Carlo simulation (FLUKA) of the 0.5 Gy irradiation, including all secondary particles without electrons (A) and the FLUKA data for carbon ions and the corresponding FNTD data acquired (B). The FLUKA simulation shows the whole LET (Linear energy transfer) spectrum of ions proton, helium, boron, beryllium, Carbon and Lithium for an area of 333x333um (a microscope FOV). The six individual graphs below show the counts expected in the 333x333 µm area per ion type. Figure B depicts the FLUKA carbon ion LET-spectra from the simulation in blue and the data from the microscopy in red. The two curves have a high degree of overlap indicating a good correlation between the simulated data and the recorded results.

Figure 5.

A representative depiction of the undefined background signal detected during imaging by WF microscopy. The two micrographs show the background signals detected while imaging the FNTD with the WF microscope. Left is an overview with a chosen area with a scale bar of 5µm on the right there is the selected segment with increased contrast and a scale bar of 2µm. The detected “snake” like pattern is above background and is present on all areas and z-layers captured.

**References**


1. Akselrod, M. and J. Kouwenberg, *Fluorescent nuclear track detectors – Review of past, present and future of the technology.* Radiation Measurements, 2018. **117**: p. 35-51.
2. Ohsawa, D., et al., *Analysis of SPICE microbeam size using fluorescent nuclear track detector (FNTD).* Nuclear Instruments and Methods in Physics Research Section B: Beam Interactions with Materials and Atoms, 2019. **453**: p. 9-14.
3. Harrison, J., et al., *CHARACTERIZATION OF FLUORESCENT NUCLEAR TRACK DETECTORS AS CRITICALITY DOSIMETERS II.* Radiation Protection Dosimetry, 2017. **180**(1-4): p. 201-205.
4. Dosanjh, M., *The changing landscape of cancer therapy*, in *CERN Courier*. 2018, CERN.
5. Niklas, M., et al., *Subcellular Spatial Correlation of Particle Traversal and Biological Response in Clinical Ion Beams.* International journal of radiation oncology, biology, physics, 2013. **87**.
6. Akselrod, M.S. and G.J. Sykora, *Fluorescent nuclear track detector technology – A new way to do passive solid state dosimetry.* Radiation Measurements, 2011. **46**(12): p. 1671-1679.
7. Osinga, J.M., et al., *High-accuracy fluence determination in ion beams using fluorescent nuclear track detectors.* Radiation Measurements, 2013. **56**: p. 294-298.
8. Niklas, M., et al., *Subcellular Spatial Correlation of Particle Traversal and Biological Response in Clinical Ion Beams.* International Journal of Radiation Oncology • Biology • Physics, 2013. **87**(5): p. 1141-1147.
9. Rahmanian, S., et al., *Application of fluorescent nuclear track detectors for cellular dosimetry.* Physics in Medicine and Biology, 2017. **62**(7): p. 2719-2740.

10. Kodaira, S., et al., *Co-visualization of DNA damage and ion traversals in live mammalian cells using a fluorescent nuclear track detector.* Journal of radiation research, 2015. **56**(2): p. 360-365.
11. McFadden, C.H., et al., *Isolation of time-dependent DNA damage induced by energetic carbon ions and their fragments using fluorescent nuclear track detectors.* Medical Physics, 2020. **47**(1): p. 272-281.
12. Niklas M, et al., *The biomedical sensor Cell-Fit-HD4D, reveals individual tumor cell fate in response to microscopic ion deposition.* BioRx, 2020.
13. Greilich, S., et al., *Fluorescent nuclear track detectors as a tool for ion-beam therapy research.* Radiation Measurements, 2013. **56**: p. 267-272.
14. Dokic, I., et al., *Correlation of Particle Traversals with Clonogenic Survival Using Cell-Fluorescent Ion Track Hybrid Detector.* Frontiers in Oncology, 2015. **5**(275).
15. Dokic, I., et al., *Next generation multi-scale biophysical characterization of high precision cancer particle radiotherapy using clinical proton, helium-, carbon- and oxygen ion beams.* Oncotarget, 2016. **7**.
16. Niklas, M., et al., *Registration procedure for spatial correlation of physical energy deposition of particle irradiation and cellular response utilizing cell-fluorescent ion track hybrid detectors.* Physics in medicine and biology, 2016. **61**: p. N441-N460.
17. Kouwenberg, J.J.M., et al., *A 3D feature point tracking method for ion radiation.* Physics in Medicine and Biology, 2016. **61**(11): p. 4088-4104.
18. Team, R., *RStudio: Integrated Development for R.* RStudio, Inc., 2015.
19. Bauer, J., et al., *Integration and evaluation of automated Monte Carlo simulations in the clinical practice of scanned proton and carbon ion beam therapy.* Physics in Medicine and Biology, 2014. **59**(16): p. 4635-4659.

Figure 1

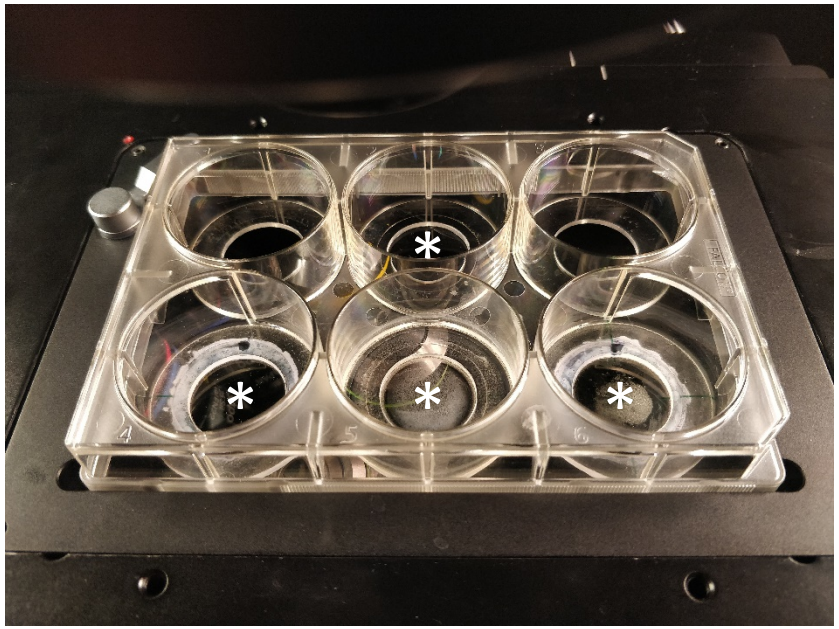


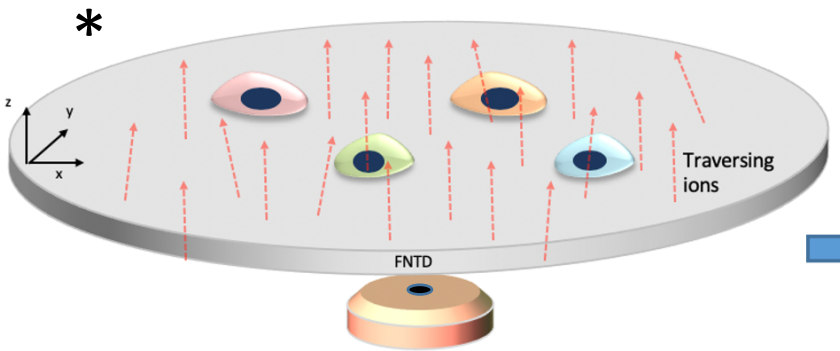


Seeding of cells and Irradiation of the FNTD

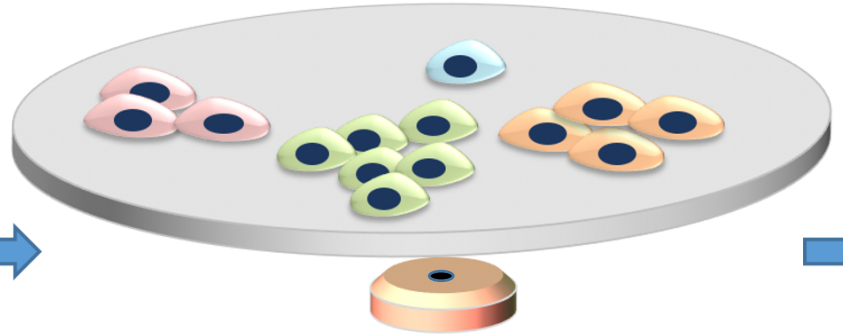

Live cell imaging of cells

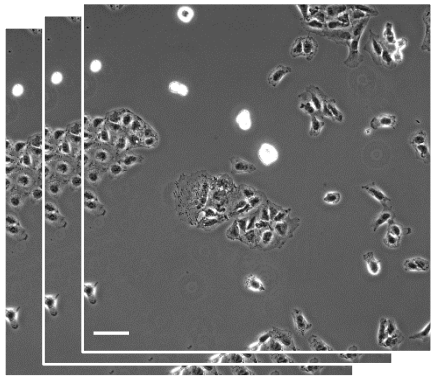

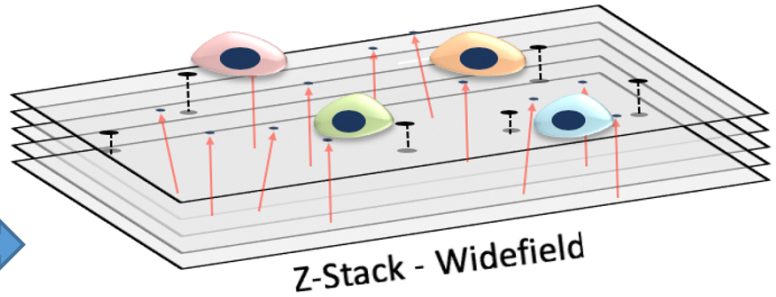


Imaging of the trackspots

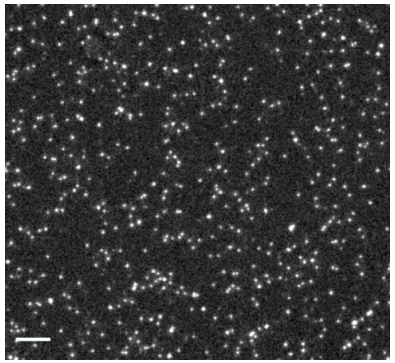

Figure 2

A

Confocal

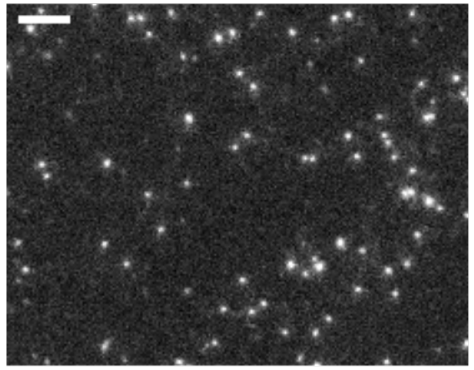

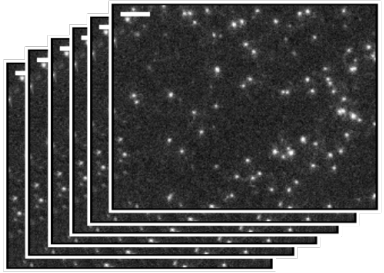

Widefield

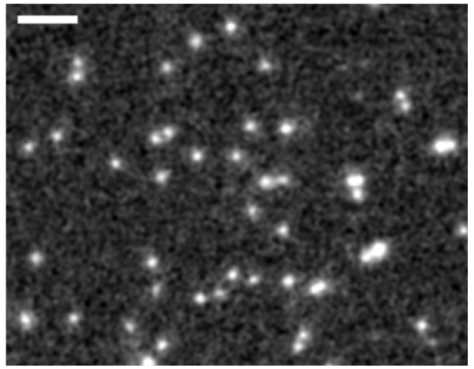

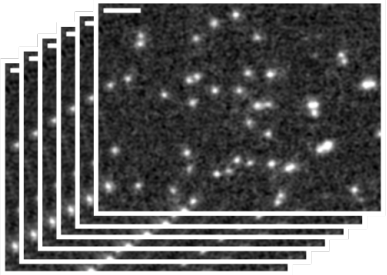

Z-stack 21 slices

| Capture time: | Capture time: |
|---|---|
| 11 min | 1min 45 sec |
| 193x193 um | 333x333 um |
| 1024x1024 px | 2048x2048 px |
| 8-bit Image | 16-bit Image |

B

Widefield 40x

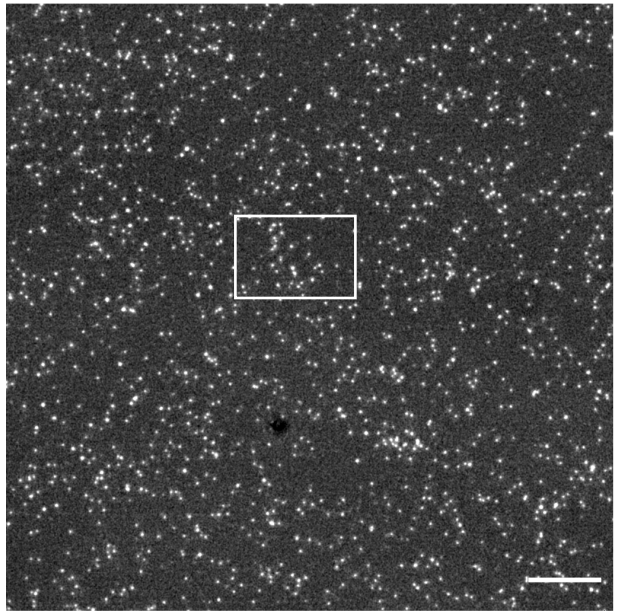

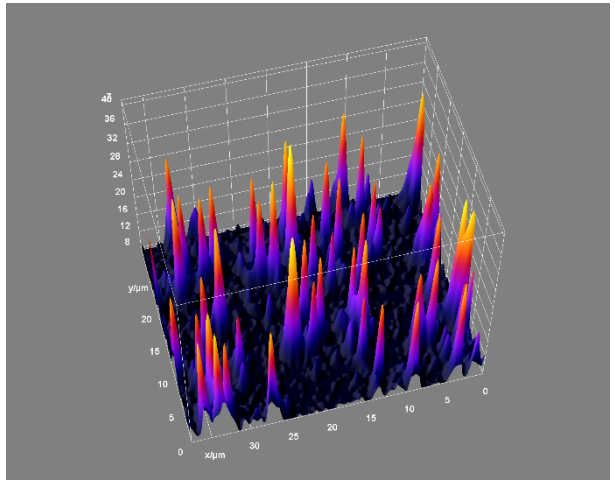

Confocal 40x

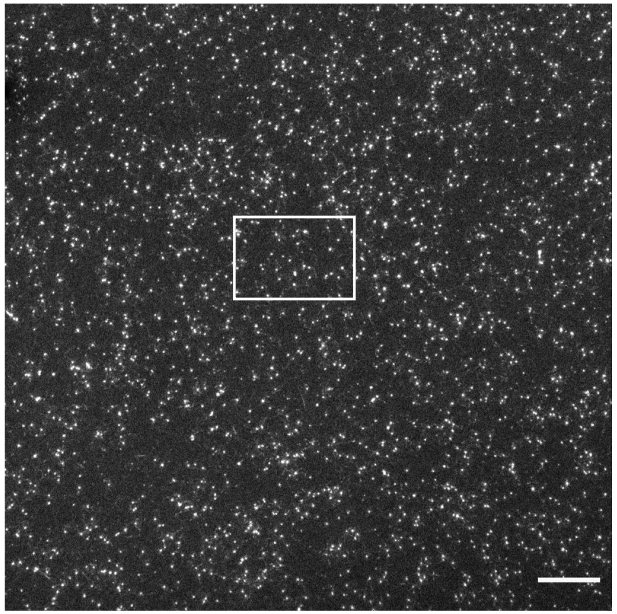

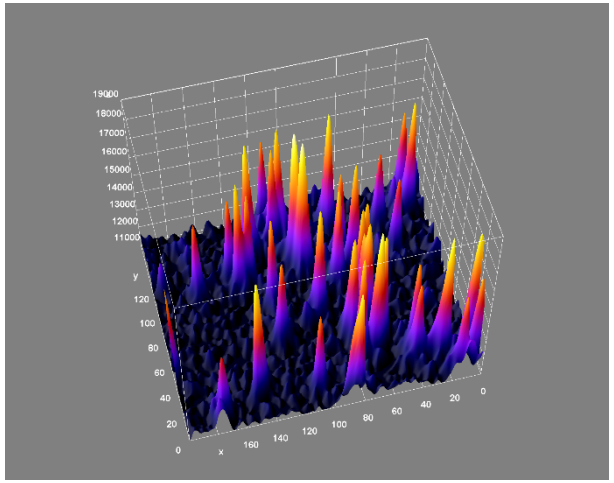

Figure 3

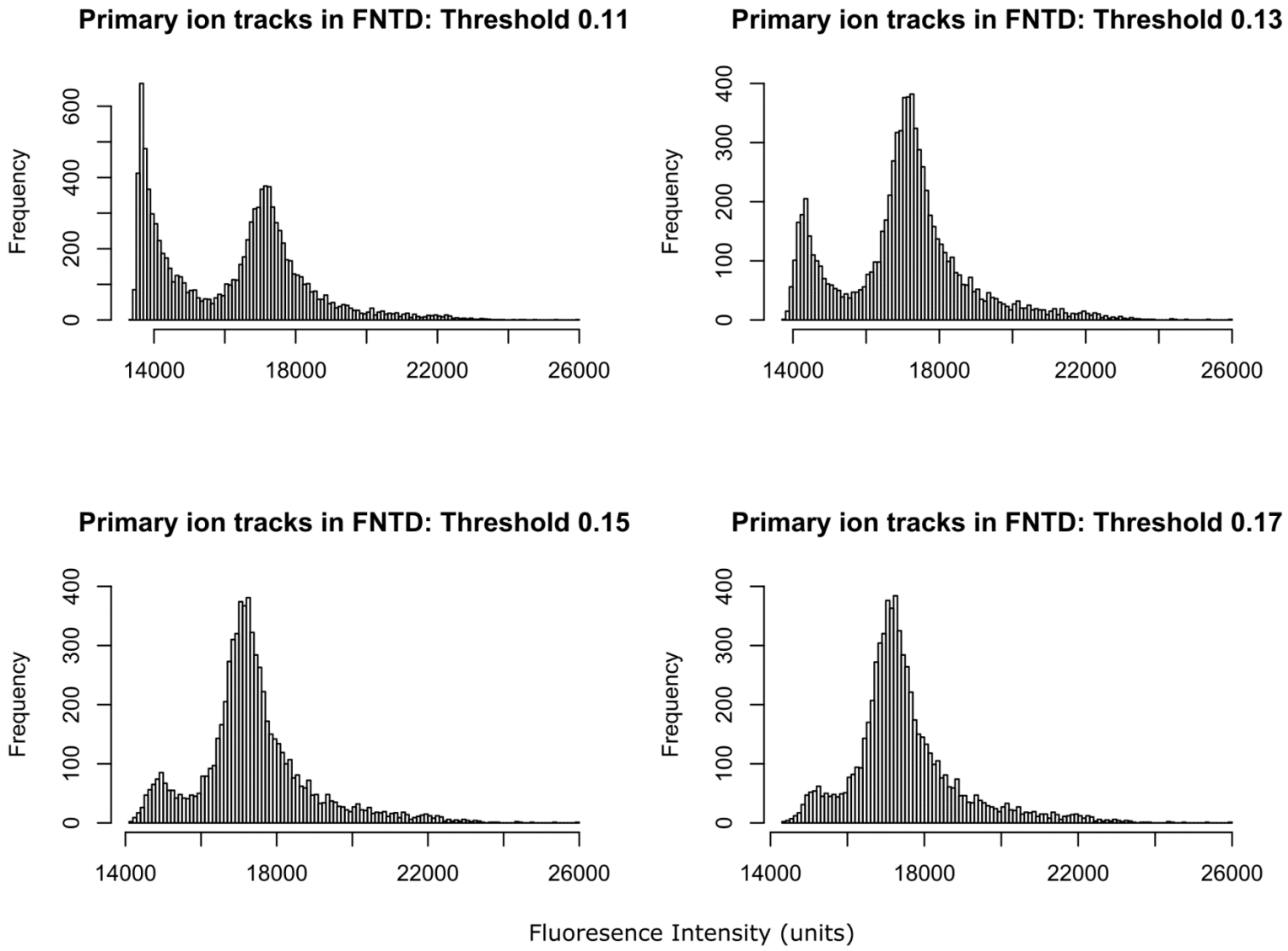
Primary ion tracks in FNTD: Threshold 0.11
Primary ion tracks in FNTD: Threshold 0.13
Primary ion tracks in FNTD: Threshold 0.15
Primary ion tracks in FNTD: Threshold 0.17
Frequency
0
100
200
300
400
600
14000
18000
22000
26000
Fluoresence Intensity (units)

Figure 4

**A**

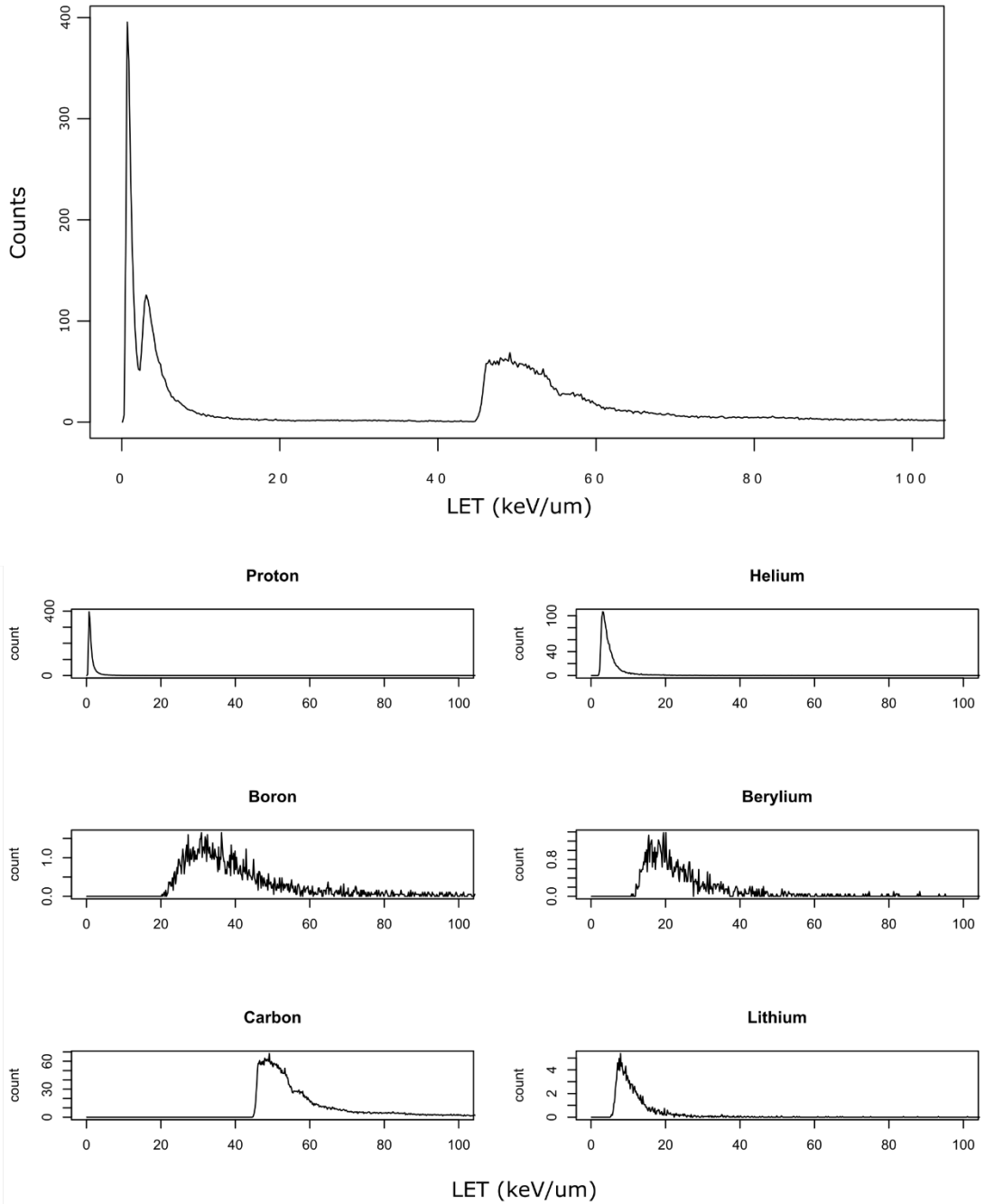
Counts
LET (keV/um)
Proton
Helium
Boron
Berylium
Carbon
Lithium
count
LET (keV/um)

**B**

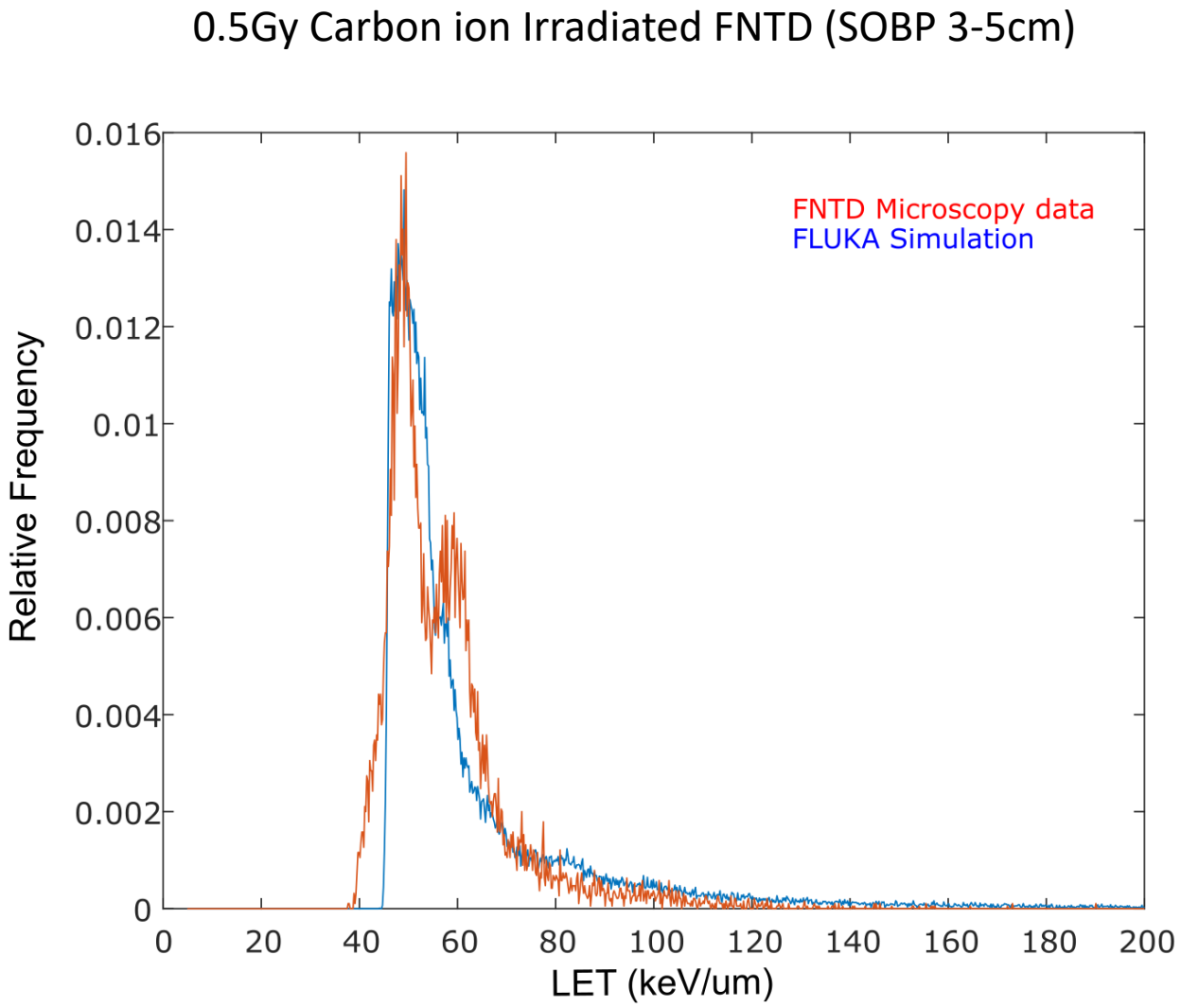
0.5Gy Carbon ion Irradiated FNTD (SOBP 3-5cm)
FNTD Microscopy data
FLUKA Simulation
Relative Frequency
LET (keV/um)
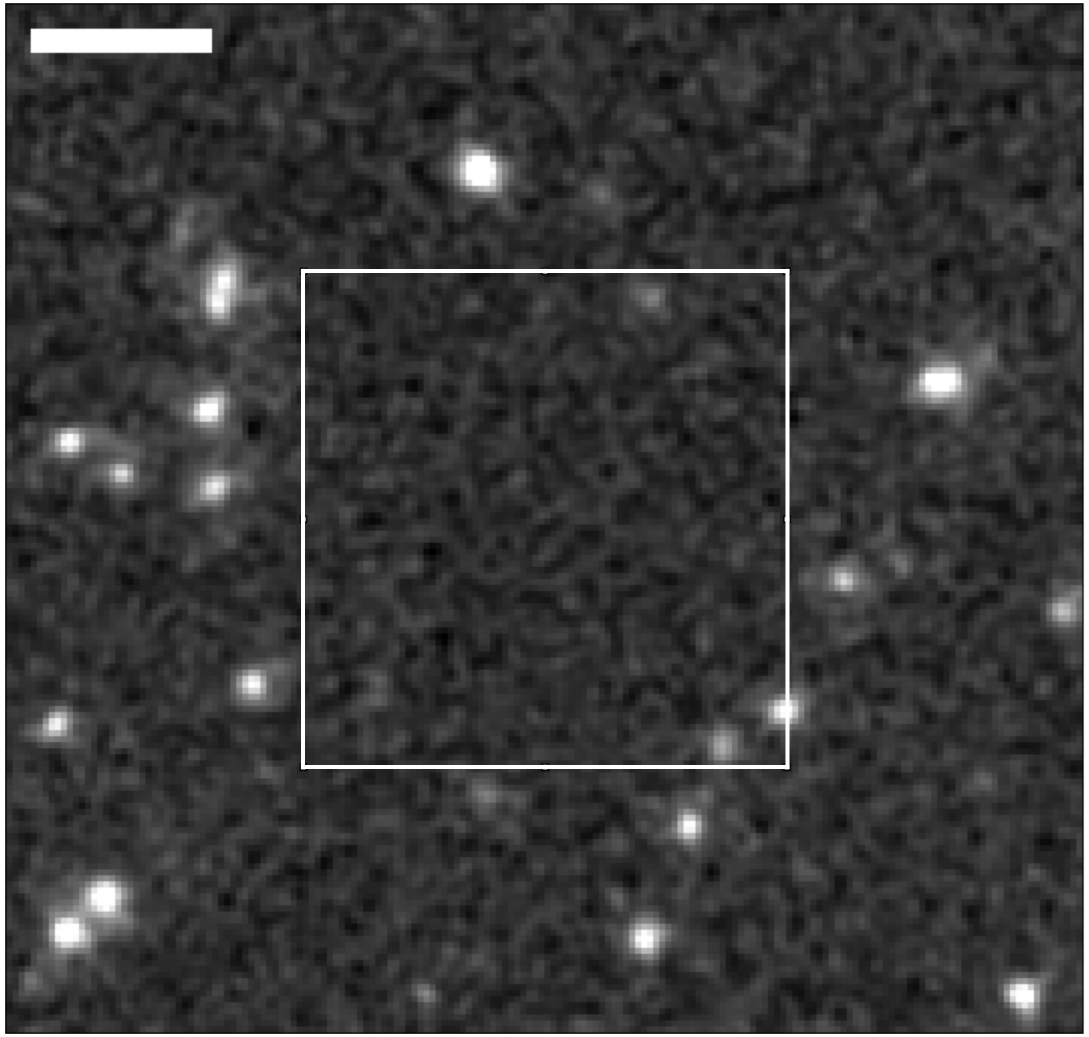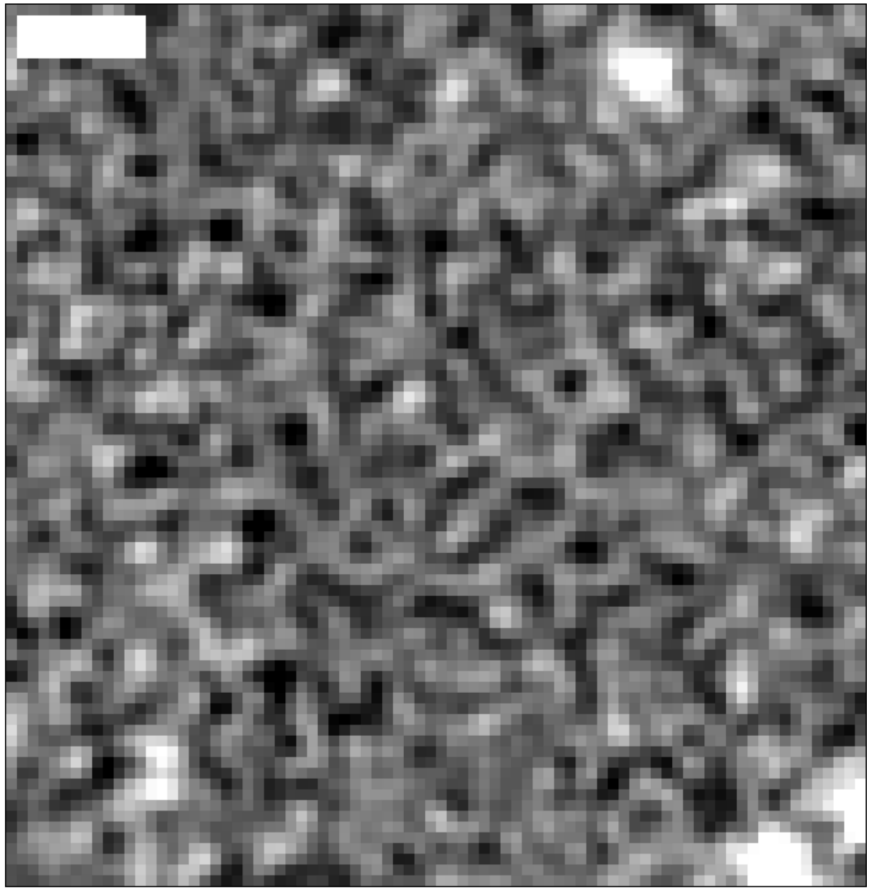
Figure 5